

Superresolution and corrections to the diffusion approximation in optical tomography

George Y. Panasyuk, Vadim A. Markel, and John C. Schotland
Departments of Bioengineering and Radiology, University of Pennsylvania, Philadelphia, Pennsylvania 19104

(Received 28 April 2005; accepted 18 July 2005; published online 1 September 2005)

We demonstrate that the spatial resolution of images in optical tomography is not limited to the fundamental length scale of one transport mean free path. This result is facilitated by the introduction of novel corrections to the standard integral equations of scattering theory within the diffusion approximation to the radiative transport equation. © 2005 American Institute of Physics. [DOI: 10.1063/1.2040010]

There has been considerable recent interest in the development of optical methods for tomographic imaging.¹ The physical problem that is considered is to recover the optical properties of the interior of an inhomogeneous medium from measurements taken on its surface. The starting point for the mathematical formulation of this inverse scattering problem (ISP) is a model for the propagation of light, typically taken to be the diffusion approximation (DA) to the radiative transport equation (RTE). The DA is valid when the energy density of the optical field varies slowly on the scale of the transport mean free path ℓ^* . The DA breaks down in optically thin layers, near boundary surfaces, or near the source. One or more of these conditions are encountered in biomedical applications such as imaging of small animals² or of functional activity in the brain.

Within the accuracy of the DA, reconstruction algorithms based on both numerical³ and analytic solutions⁴⁻⁶ to the ISP have been described. Regardless of the method of inversion, the spatial resolution of reconstructed images is expected to be limited to ℓ^* . This expectation is due to the intertwined effects of the ill-posedness of the ISP⁵ and intrinsic inaccuracies of the DA.⁷ In this letter, we introduce novel corrections to the integral equations of scattering theory within the DA. Using this result, we report the reconstruction of superresolved images whose spatial resolution is less than ℓ^* .

We begin by considering the propagation of multiply scattered light in an inhomogeneous medium characterized by an absorption coefficient $\mu_a(\mathbf{r})$. In what follows, we will neglect the contribution of ballistic photons and consider only diffuse photons whose specific intensity $I(\mathbf{r}, \hat{\mathbf{s}})$ at the point \mathbf{r} in the direction $\hat{\mathbf{s}}$ is taken to obey the time-independent RTE

$$\hat{\mathbf{s}} \cdot \nabla I(\mathbf{r}, \hat{\mathbf{s}}) + (\mu_a + \mu_s)I(\mathbf{r}, \hat{\mathbf{s}}) - \mu_s \int d^2s' A(\hat{\mathbf{s}}, \hat{\mathbf{s}}') I(\mathbf{r}, \hat{\mathbf{s}}') = S(\mathbf{r}, \hat{\mathbf{s}}), \quad (1)$$

where μ_s is the scattering coefficient, $A(\hat{\mathbf{s}}, \hat{\mathbf{s}}')$ is the scattering kernel, and $S(\mathbf{r}, \hat{\mathbf{s}})$ is the source. The change in specific intensity due to spatial fluctuations in $\mu_a(\mathbf{r})$ can be obtained from the integral equation

$$\phi(\mathbf{r}_1, \hat{\mathbf{s}}_1; \mathbf{r}_2, \hat{\mathbf{s}}_2) = \int d^3r d^2s G(\mathbf{r}_1, \hat{\mathbf{s}}_1; \mathbf{r}, \hat{\mathbf{s}}) G(\mathbf{r}, \hat{\mathbf{s}}; \mathbf{r}_2, \hat{\mathbf{s}}_2) \delta\mu_a(\mathbf{r}). \quad (2)$$

Here the data function $\phi(\mathbf{r}_1, \hat{\mathbf{s}}_1; \mathbf{r}_2, \hat{\mathbf{s}}_2)$ is proportional, to lowest order in $\delta\mu_a$, to the change in specific intensity relative to a reference medium with absorption μ_a^0 . G is the Green's function for Eq. (1) with $\mu_a = \mu_a^0$, $\delta\mu_a(\mathbf{r}) = \mu_a(\mathbf{r}) - \mu_a^0$. $\mathbf{r}_1, \hat{\mathbf{s}}_1$ and $\mathbf{r}_2, \hat{\mathbf{s}}_2$ denote the position and direction of a unidirectional point source and detector, respectively.

We now show that the integral equation Eq. (2) may be used to obtain corrections to the usual formulation of scattering theory within the DA. To proceed, we note that, following Ref. 6, the Green's function $G(\mathbf{r}, \hat{\mathbf{s}}; \mathbf{r}', \hat{\mathbf{s}}')$ may be expanded in angular harmonics of $\hat{\mathbf{s}}$ and $\hat{\mathbf{s}}'$

$$G(\mathbf{r}, \hat{\mathbf{s}}; \mathbf{r}', \hat{\mathbf{s}}') = \frac{c}{4\pi} (1 + \ell^* \hat{\mathbf{s}} \cdot \nabla_{\mathbf{r}}) (1 - \ell^* \hat{\mathbf{s}}' \cdot \nabla_{\mathbf{r}'}) G(\mathbf{r}, \mathbf{r}'), \quad (3)$$

where $\ell^* = 1/[\mu_a^0 + \mu_s']$ with $\mu_s' = (1-g)\mu_s$, g being the anisotropy of the scattering kernel A . The Green's function $G(\mathbf{r}, \mathbf{r}')$ satisfies the diffusion equation $(-D_0 \nabla^2 + \alpha_0)G(\mathbf{r}, \mathbf{r}') = \delta(\mathbf{r} - \mathbf{r}')$, where the diffusion coefficient $D_0 = 1/3c\ell^*$ and $\alpha_0 = c\mu_a^0$. In addition, the Green's function must satisfy boundary conditions on the surface of the medium (or at infinity in the case of free boundaries). In general, we will consider boundary conditions of the form $G(\mathbf{r}, \mathbf{r}') + \ell \hat{\mathbf{n}} \cdot \nabla G(\mathbf{r}, \mathbf{r}') = 0$, where $\hat{\mathbf{n}}$ is the outward unit normal to the surface bounding the medium and ℓ is the extrapolation distance. Equation (3) may be seen to correspond to the first term of the P_N expansion for the Green's function of the RTE. It is possible to carry out this expansion to higher order as was done in Ref. 8, where a finite-element based iterative reconstruction algorithm was developed.

Making use of Eq. (3) and performing the angular integration over $\hat{\mathbf{s}}$ in Eq. (2) we obtain

$$\phi(\mathbf{r}_1, \hat{\mathbf{s}}_1; \mathbf{r}_2, \hat{\mathbf{s}}_2) = \frac{c}{4\pi} \Delta_1 \Delta_2 \int d^3r \left[G(\mathbf{r}_1, \mathbf{r}) G(\mathbf{r}, \mathbf{r}_2) - \frac{\ell^{*2}}{3} \nabla_{\mathbf{r}} G(\mathbf{r}_1, \mathbf{r}) \cdot \nabla_{\mathbf{r}} G(\mathbf{r}, \mathbf{r}_2) \right] \delta\alpha(\mathbf{r}), \quad (4)$$

where the differential operators $\Delta_k = 1 - (-1)^k \ell^* \hat{\mathbf{s}}_k \cdot \nabla_{\mathbf{r}_k}$ with $k=1, 2$ and $\delta\alpha = c \delta\mu_a$. Note that if the source and detector

are oriented in the inward and outward normal directions, respectively, then Eq. (4) becomes

$$\begin{aligned} \phi(\mathbf{r}_1, -\hat{\mathbf{n}}(\mathbf{r}_1); \mathbf{r}_2, \hat{\mathbf{n}}(\mathbf{r}_2)) \\ = \frac{c}{4\pi} \left(1 + \frac{\ell^*}{\ell}\right)^2 \int d^3r \left[G(\mathbf{r}_1, \mathbf{r}) G(\mathbf{r}, \mathbf{r}_2) \right. \\ \left. - \frac{\ell^{*2}}{3} \nabla_{\mathbf{r}} G(\mathbf{r}_1, \mathbf{r}) \cdot \nabla_{\mathbf{r}} G(\mathbf{r}, \mathbf{r}_2) \right] \delta\alpha(\mathbf{r}), \end{aligned} \quad (5)$$

where we have used the boundary conditions on G to evaluate the action of the Δ_k operators. Equation (5) is the main theoretical result of this letter. It may be viewed as providing corrections to the DA since the first term on the right hand side of Eq. (5) corresponds to the standard DA in an inhomogeneous absorbing medium. We note that the second term may be interpreted as defining an effective diffusion coefficient $D(\mathbf{r}) = D_0 - (\ell^{*2}/3)\delta\alpha(\mathbf{r})$ since the expression $\nabla_{\mathbf{r}} G(\mathbf{r}_1, \mathbf{r}) \cdot \nabla_{\mathbf{r}} G(\mathbf{r}, \mathbf{r}_2)$ defines the diffusion kernel in a medium with an inhomogeneous diffusion coefficient.³

For the remainder of this letter we will work in the planar measurement geometry, often encountered in small-animal imaging. In this case, Eq. (4) becomes

$$\phi(\boldsymbol{\rho}_1, \boldsymbol{\rho}_2) = \int d^3r K(\boldsymbol{\rho}_1, \boldsymbol{\rho}_2; \mathbf{r}) \delta\alpha(\mathbf{r}), \quad (6)$$

where $\boldsymbol{\rho}_1$ denotes the transverse coordinates of a point source in the plane $z=0$, $\boldsymbol{\rho}_2$ denotes the transverse coordinates of a point detector in the plane $z=L$, and the dependence of ϕ on $\hat{\mathbf{s}}_1$ and $\hat{\mathbf{s}}_2$ is not made explicit. Evidently, from considerations of invariance of the kernel $K(\boldsymbol{\rho}_1, \boldsymbol{\rho}_2; \mathbf{r})$ under translations of its transverse arguments, it can be seen that K may be expressed as the Fourier integral

$$\begin{aligned} \kappa(\mathbf{q}_1, \mathbf{q}_2; z) = \frac{c}{16\pi D_0^2 Q(\mathbf{q}_1) Q(\mathbf{q}_2)} \left[1 + \frac{\ell^{*2}}{3} (Q(\mathbf{q}_1) Q(\mathbf{q}_2) - \mathbf{q}_1 \cdot \mathbf{q}_2) \right] \\ \times \exp[-Q(\mathbf{q}_1)|z| - Q(\mathbf{q}_2)|z-L|], \end{aligned} \quad (7)$$

where $Q(\mathbf{q}) = (q^2 + \alpha_0/D_0)^{1/2}$ and we have assumed that $\hat{\mathbf{s}}_1 = \hat{\mathbf{s}}_2 = \hat{\mathbf{z}}_1$.

Inversion of the integral equation Eq. (6) may be carried out by analytic methods. These methods have been shown to be computationally efficient and may be applied to data sets consisting of a very large number of measurements.^{5,6} The approach taken is to construct the singular value decomposition of the linear operator K in the proper Hilbert space setting and then use this result to obtain the pseudoinverse solution to Eq. (6). In this manner, it is possible to account for the effects of sampling and thereby obtain the best (in the sense of minimizing the appropriate L^2 norm) bandlimited approximation to $\delta\alpha$. Here we use this approach to simulate

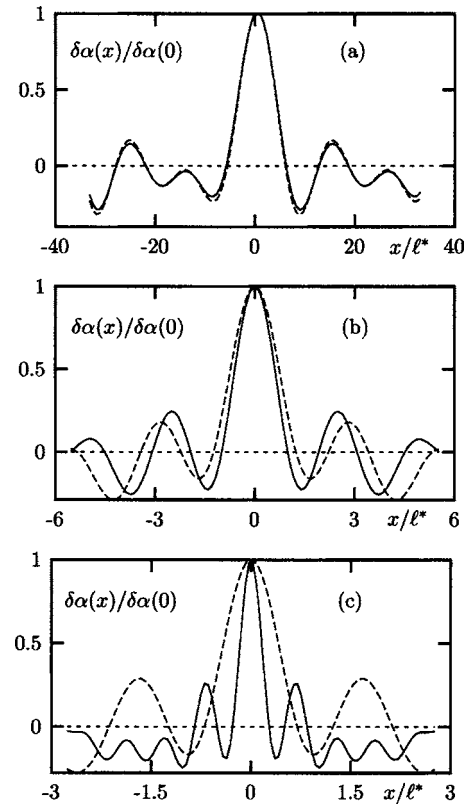


FIG. 1. Reconstructions of a point absorber for different thicknesses of the slab using the corrected (solid curve) and uncorrected (dashed curve) DA.

$$\begin{aligned} K(\boldsymbol{\rho}_1, \boldsymbol{\rho}_2; \mathbf{r}) = \frac{1}{(2\pi)^4} \int d^2q_1 d^2q_2 \kappa(\mathbf{q}_1, \mathbf{q}_2; z) \\ \times \exp[i(\mathbf{q}_1 - \mathbf{q}_2) \cdot \boldsymbol{\rho} - i(\mathbf{q}_1 \cdot \boldsymbol{\rho}_1 - \mathbf{q}_2 \cdot \boldsymbol{\rho}_2)], \end{aligned}$$

where $\mathbf{r} = (\boldsymbol{\rho}, z)$. The function κ may be obtained from the plane-wave expansion of the diffusion Green's function obeying appropriate boundary conditions. In the case of free boundaries, it is readily seen that κ is given by the expression

the reconstruction of a point absorber located at a point \mathbf{r}_0 between the measurement planes with $\delta\alpha(\mathbf{r}) = A\delta(\mathbf{r} - \mathbf{r}_0)$ for constant A . In this situation it is possible to calculate the data function ϕ within radiative transport theory, thus avoiding "inverse crime." To proceed, we require the Green's function $G(\mathbf{r}, \hat{\mathbf{s}}; \mathbf{r}', \hat{\mathbf{s}}')$ for the RTE in a homogeneous infinite medium which we obtain as described in Ref. 9. Note that in this case, the angular integration over $\hat{\mathbf{s}}$ in Eq. (2) may be carried out analytically.

The effects of corrections to the DA were studied in numerical simulations following the methods of Ref. 5. The simulations were performed for a medium with optical properties similar to breast tissue in the near infrared.¹⁰ The back-

ground absorption and reduced scattering coefficients were given by $\mu_a^0=0.03\text{ cm}^{-1}$ and $\mu_s'=10\text{ cm}^{-1}$. The scattering kernel was taken to be of Henyey-Greenstein-type with $A(\hat{s},\hat{s}')=\sum_{\ell=0}^{\infty}g^{\ell}P_{\ell}(\hat{s}\cdot\hat{s}')$ and $g=0.98$. This choice of parameters corresponds to $\ell^*=1\text{ mm}$ and $D_0=0.8\text{ cm}^2\text{ ns}^{-1}$. The separation between the measurement planes L was varied in order to explore the effects of the corrections. A single point absorber was placed at the midpoint of the measurement planes with $\mathbf{r}_0=(0,0,L/2)$ and $A=1\text{ cm}^3\text{ ns}^{-1}$. The sources and detectors were located on a square lattice with spacing h . The total number of source-detector pairs N was varied, along with h , as indicated below. To demonstrate the stability of the reconstruction in the presence of noise, Gaussian noise of zero mean was added to the data at the 1% level, relative to the average signal. Note that the level of regularization was chosen to be the same for all reconstructions.

Reconstruction of $\delta\alpha(\mathbf{r})$ for a point absorber defines the point spread function (PSF) of the reconstruction algorithm. The resolution Δx is defined as the half width at half maximum of the PSF. In Fig. 1(a) we consider the case of a thick layer with $L=6.6\text{ cm}$. The above parameters were chosen to be $h=0.83\text{ mm}$ and $N=1.5\times 10^9$. PSFs with and without corrections are shown. It may be seen that the effect of the corrections is negligible in the case of a thick layer and the resolution $\Delta x=3.5\ell^*$. For the case of a layer of intermediate thickness with $L=1.1\text{ cm}$, as shown in Fig. 1(b), the corrections have a more significant effect. In particular, with $h=0.28\text{ mm}$ and $N=1.2\times 10^{11}$, we found that $\Delta x=0.9\ell^*$ for the uncorrected reconstruction and $\Delta x=0.7\ell^*$ for the corrected reconstruction. The corrections are most significant for the thinnest layer considered in this study, achieving a factor of 2 improvement in resolution when $L=0.55\text{ cm}$. In this case, with $h=0.14\text{ mm}$ and $N=1.9\times 10^{12}$, we found that $\Delta x=0.4\ell^*$ for the uncorrected case and $\Delta x=0.2\ell^*$ for the corrected case as shown in Fig. 1(c). We note that the curves in Fig. 1(a) are not symmetric about their central maxima, whereas those in Figs. 1(b) and 1(c) appear to be symmetric. The explanation for this result is that the inverse problem for the thick layer is more ill posed than in the case of the thin-

ner layers due to the exponential decay of the diffuse wave. In the absence of noise, the PSF for the thick layer also appears to be symmetric (graph not shown).

In conclusion, we have described a series of corrections to the usual formulation of the DA in optical tomography. We have found that these corrections give rise to superresolved images with resolution below ℓ^* . Several comments on these results are necessary. First, the effects of corrections were demonstrated to be most significant in optically thin layers. However, corrections to the DA may also be expected to be important for thick layers when inhomogeneities in the absorption are located near the surface. Second, the results of this study were obtained without resorting to so-called inverse crime. That is, forward scattering data were obtained from the full RTE under conditions when the DA is known to break down. Third, the use of analytic reconstruction algorithms was essential for handling the extremely large data sets employed in this study. Note that such data sets may be obtained in modern noncontact optical tomography systems.¹¹ Finally, we note that higher order corrections to the DA are also expected to be important for the nonlinear ISP.

This research was supported by the NIH under the Grant No. P41RR02305 and by the AFOSR under Grant No. F41624-02-1-7001.

¹A. Gibson, J. Hebden and S. Arridge, *Phys. Med. Biol.* **50**, R1 (2005).

²E. E. Graves, J. Ripoll, R. Weissleder, and V. Ntziachristos, *Med. Phys.* **30**, 901 (2003).

³S. Arridge, *Inverse Probl.* **15**, R41 (1999).

⁴J. C. Schotland, *J. Opt. Soc. Am. A* **14**, 275 (1997).

⁵V. A. Markel and J. C. Schotland, *Appl. Phys. Lett.* **81**, 1180 (2002).

⁶V. A. Markel and J. C. Schotland, *Phys. Rev. E* **70**, 056616 (2004).

⁷K. Yoo, F. Liu, and R. Alfano, *Phys. Rev. Lett.* **65**, 2210 (1990).

⁸H. Jiang, *Opt. Express* **4**, 241 (1999).

⁹V. A. Markel, *Waves Random Media* **14**, L13 (2004).

¹⁰V. Peters, D. Wyman, M. Patterson, and G. Frank, *Phys. Med. Biol.* **35**, 1317 (1990).

¹¹J. Ripoll and V. Ntziachristos, *Mod. Phys. Lett. B* **18**, 1403 (2004).